

LINEAR AND NONLINEAR DEFORMATION EFFECTS IN THE PERMANENT GNSS NETWORK OF CYPRUS

C. Danezis¹, M. Chatzinikos², C. Kotsakis³

¹Dept. of Civil Engineering and Geomatics, Cyprus University of Technology, (chris.danezis@cut.ac.cy)

²Dept. of Geodesy and Surveying, Aristotle University of Thessaloniki, (mchatzin@topo.auth.gr)

³Dept. of Geodesy and Surveying, Aristotle University of Thessaloniki, (kotsaki@topo.auth.gr)

Key words: *GNSS geodesy; position time series; station velocities; seasonal variations; Cyprus*

ABSTRACT

Since 2008, CYPOS, a geodetic network of seven permanent GNSS stations is operating in the island of Cyprus under the auspices of the Department of Lands and Surveys (DLS). The network covers the government controlled areas, with inter-station distances of about 60 km, and it supports the needs for various surveying and geodetic engineering applications. The continuous character of positioning data that are collected over this network offer useful information to investigate the behaviour of the crustal deformation field in Cyprus, yet no relevant studies have been performed up to now. This paper presents the results of a multi-year analysis (11/2011-01/2017) of daily GNSS data in the aforementioned network, and it provides inferences of linear and nonlinear deforming signals into the position time series of the network stations. In particular, 3D station velocities and seasonal (annual) periodic displacements are jointly estimated via a data stacking approach with respect to the IGB08 reference frame.

I. INTRODUCTION

A. GNSS networks and position time series in the study of crustal deformations

The use of permanent Global Navigation Satellite Systems (GNSS) networks offers the potential to continuously observe the motion of Earth-fixed stations. This allows us to monitor crustal displacements through the analysis of position time series derived from daily or weekly GNSS network adjustments under identical processing options for each session solution. In general, the temporal variations that appear in the position time series of permanent GNSS stations, either in the horizontal or vertical spatial components, are associated with four main sources:

- i) true Earth deformation due to various geophysical phenomena, such as lithospheric tectonic displacements in global or regional scale (Sella et al., 2002; Altamimi et al., 2012; Reilinger et al., 2006), post-glacial rebound (King et al., 2010), ocean loading (Vey et al., 2002), atmospheric pressure loading (Dach et al., 2010);
- ii) GNSS-related observational or modeling errors, like multipath (King and Watson, 2010; Goebell and King, 2011), orbital errors (Steigenberger et al., 2009) and inefficient atmospheric models (Munekane and Boehm, 2010);
- iii) sudden geophysical or non-geophysical events, such as position discontinuities due to antenna change (Williams, 2003; Perfetti, 2006), antenna calibration model switch (Chatzinikos et al., 2009) and co-seismic displacements (Ostini, 2012; Chatzinikos 2013);

iv) temporal variations of the reference frame that is used in the description of position time series (Altamimi and Dermanis, 2012; Chatzinikos and Dermanis, 2015).

Two of the most important signals that are regularly modeled in the analysis of position time series is their long-term (secular) linear trend due to constant station velocities, and their nonlinear evolution due to the presence of seasonal (periodic or quasi-periodic) variations with constant or time-dependent signal amplitude and phase. The linear part is of great interest for geodynamical studies as it represents the dominating effects caused by tectonic plate motion and post-glacial rebound on the horizontal and vertical station displacements, respectively. The well known Euler pole model with constant angular velocity is a common tool for describing the (horizontal part of the) secular displacements as a circular motion of plate-fixed points over the Earth's surface. Within the limited time span of a few decades, the circular plate motion is sufficiently approximated in terms of constant station velocities with respect to a Cartesian terrestrial reference frame, such as the ITRF (Altamimi et al., 2012). Note however that tectonic plate motions may also occur around migrating Euler poles with varying angular velocity.

The nonlinear part in GNSS position time series originating from seasonal signals with annual and/or semi-annual periods is not totally understood (Dong et al., 2002; Penna et al., 2007), yet a significant portion of them should be attributed to the influence of Earth loading effects that remain unmodeled during the GNSS data processing (van Dam et al., 1994; van Dam and Wahr, 1998). Moreover, the seasonal variations in

position time series do not always have a strictly periodic character, a fact which indicates the presence of yearly disturbances in their associated geophysical sources within the dynamic Earth system.

B. Aim of the study

The scope of this paper is to present the results from the daily and multi-year processing of continuous GNSS data at the seven permanent GNSS stations of CYPOS. These stations are shown in Figure 1 and they currently provide the skeleton of the national geodetic network for GNSS-based applications in Cyprus. The analysis of linear and nonlinear temporal variations in their position time series, which is performed herein for the first time, will provide useful insight on the deformation characteristics of CYPOS.

The used observations cover a time period of more than five years (30/11/2011-28/01/2017) and they were processed along with daily RINEX data from thirty-five stations of the European Permanent Network (EPN, Bruyninx et al., 2012) including the NICO station which is located in Nicosia. For the daily and multi-year adjustment of the GNSS data we have used the Bernese software package, version 5.2 (Dach et al., 2015). Additional software developed at the Department of Geodesy and Surveying of the Aristotle University of Thessaloniki was used to compute specific quality metrics for the daily and multi-year GNSS solutions, as well as for the least-squares fittings of seasonal models to the position time series.

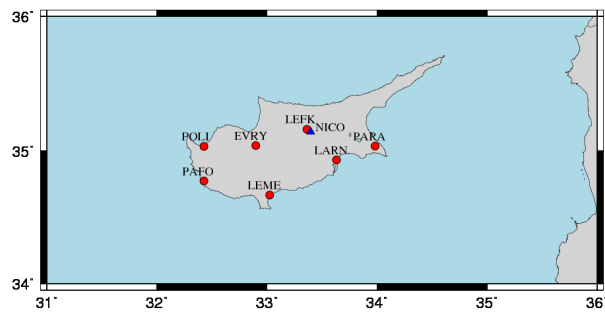


Figure 1. The permanent GNSS network of Cyprus (CYPOS); red circles indicate the seven stations whose position time series are analyzed in this paper.

The main products of this work consist of: (a) the estimated geocentric Cartesian coordinates (at epoch $t=2005.0$) and velocities of the seven GNSS stations with respect to the IGB08 frame (Rebischung et al., 2011), and (b) their residual position time series, after the removal of the velocity-based trends, with respect to the local topocentric system of each station (East, North, Up components). Both of the above products have been further analyzed to infer the local deformation field in the network of CYPOS and the presence of seasonal signals in the respective time series of the network stations. In the following sections of the paper we present in detail the main findings in relation to this analysis.

II. PROCESSING OF CONTINUOUS GNSS DATA

A. Daily Solutions

The overall network that was formed for computing the daily solutions consists in total of forty-two stations. Besides the seven GNSS stations of CYPOS, the formed network includes thirty-five selected EPN stations whose geographical distribution is shown in Figure 2. Note that the stations marked in blue represent the reference EPN stations which were employed for the datum definition in the daily and multi-year GNSS solutions.

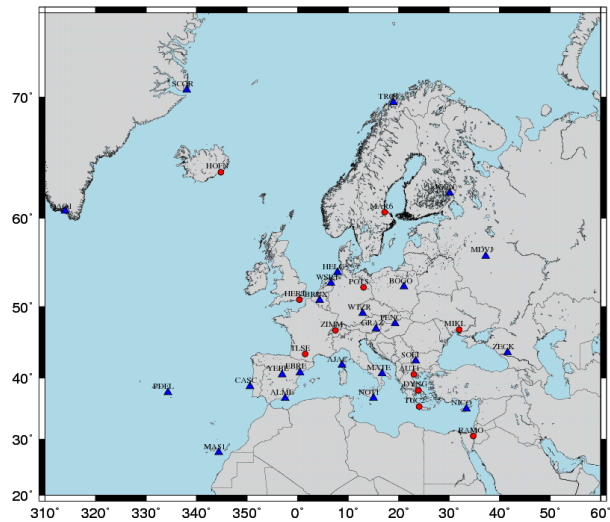


Figure 2. Map of EPN stations used in GNSS data processing.

A summary of the main options that were used during the GNSS data processing in the aforementioned network with the Bernese software is given in Table 1. The datum fixation for the daily solutions was implemented by the no-net-translation (NNT) condition to the known IGB08 coordinates of twenty-four EPN (Class-A) stations; see Figure 2. The results from this pre-processing step to be exploited in the subsequent analysis include (a) the daily station positions and their respective formal errors, and (b) the full covariance matrices of all daily network solutions. The number of participating stations in each daily solution ranges from a minimum of 27 up to a maximum of 42.

After computing each daily solution, a 7-parameter Helmert transformation was applied between the estimated daily positions and the official IGB08 positions at the twenty-four EPN reference stations. This was done to detect “problematic” reference stations that had to be excluded from the datum definition process in the respective daily solutions. Such a screening procedure was iteratively implemented until no problematic reference stations were dictated by the post-fit residuals of the daily Helmert transformations.

Table 1. Selected options for GNSS data processing

Basic observable	GNSS carrier phase. Code only for receiver clock sync and ambiguity resolution. Melbourne-Wubbena widelane method.
Elevation cut-off angle	10 deg., elevation-dependent weighting (cosz).
Data sampling	30 sec and 180 sec in final solution.
Modeled observable	Ionosphere-free linear combination of double-difference carrier phase.
Ground/satellite APC calibration	Absolute antenna phase centre corrections (igs08.atx).
Tidal displacements	IERS 2010 conventions (solid earth tides). FES 2004 (ocean loading corrections). No atmospheric loading corrections.
Satellite/receiver clock	Satellite clock biases eliminated by double-differences. Receiver clock corrections estimated in pre-processing using code observations.
Orbits and ERPs	IGS final GPS/GLONASS orbits & ERPs.
Ionosphere	First-order ionosphere delays eliminated by forming ionosphere-free L1/L2 linear combination. Higher-order ionosphere corrections are applied. Regional ionosphere maps were used to increase the number of resolved ambiguities in the QIF, L5/L3 and L1/L2 ambiguity resolution.
Ambiguity resolution	Ambiguities are resolved in baseline-by-baseline mode: Melbourne-Wubbena approach (< 6000 km) Quasi-Ionosphere-Free (QIF) approach (<2000 km) Phase-based widelane/narrowlane method (<200 km) Direct L1/L2 method, also for GLONASS (<20 km) GLONASS is considered for ambiguity resolution (<2000 km).
Troposphere	Dry GMF (prior model), estimation of hourly zenith delay corrections for each station using Wet GMF. Horizontal gradient parameter estimated/day/station (Chen-Herring).
Reference frame	IGb08, no-net translation conditions on reference station coordinates and velocities (IGb08.snx)

As an example of the quality metrics for the final daily solutions, the a-posteriori variance factor obtained by each daily network adjustment is shown in Figure 3.

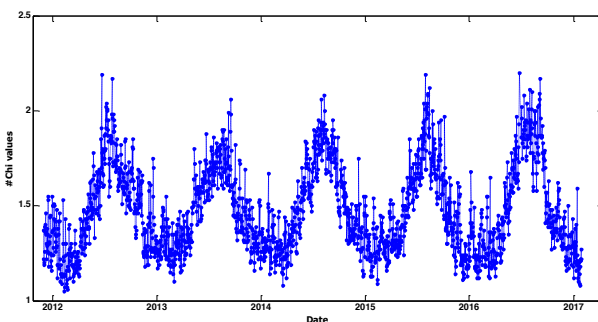


Figure 3. Daily a-posteriori variance factors in the analyzed GNSS network.

B. Multi-year solution

After the computation of all daily solutions, a multi-year adjustment was performed based on the stacking of the (unconstrained) daily normal equations. The reference frame for the multi-year solution is IGb08 and it was enforced through the NNT condition on the positions and velocities of 24 EPN (Class A) reference stations; see Figure 2. The reference epoch for the estimated positions was set to $t_0=2005.0$, similarly to the reference epoch of the official IGb08 frame. The main products from this processing step were the station positions (at t_0) and velocities of the CYPOS GNSS stations, along with their respective time series of position residuals.

In the initial computation of the multi-year solution, no station discontinuities were incorporated into the least squares stacking of the daily NEQ. From the residual time series of this first solution, eleven station discontinuities were detected by the Bernese software and they were subsequently modeled for computing the final multi-year solution. The official list of EPN station discontinuities includes six additional discontinuity events that are relevant to our network configuration for the time period of this study (11/2011-01/2017) – these were also included in the final computation of the multi-year solution. Note that, out of the total seventeen station discontinuities, two of them occurred at CYPOS stations (LEFK, PAFO) for which particular mention is given later in the paper.

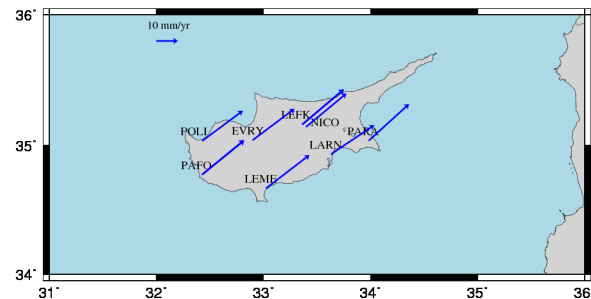


Figure 4. Estimated horizontal velocities at the CYPOS GNSS stations in IGb08.

The results of the multi-year solution for the estimated positions and velocities at the CYPOS GNSS stations are summarized in Tables 2 and 3, respectively. The stations LEFK and PAFO appear with different “validity periods” for their respective results due to the detected discontinuities as previously mentioned. The horizontal components of the estimated velocities are plotted in Figure 4. The vertical component of the estimated velocities are mostly negligible (< 1 mm/yr), with the exception of LARN and, to a lesser extent, PAFO. The first of these stations appears to have a significant downward trend of about 5 mm/yr which needs to be further investigated regarding its cause.

Table 2. Estimated positions at epoch $t_0=2005.0$ of the CYPOS GNSS stations in IGb08 (values in m).

	Validity period	X (t ₀)	Y (t ₀)	Z (t ₀)
EVRY	A	4389846.035	2839909.319	3641645.008
LARN	A	4358623.310	2899369.048	3631599.949
LEFK	B	4360035.737	2870860.968	3652605.816
	C	4360035.736	2870860.987	3652605.816
LEME	A	4403058.471	2862122.638	3607630.266
NICO	A	4359415.715	2874117.069	3650777.829
PAFO	D	4427028.128	2812497.092	3617359.846
	E	4427028.124	2812497.091	3617359.841
PARA	A	4335378.631	2922300.281	3641064.127
POLI	A	4413130.062	2803627.159	3640911.041

Table 3. Estimated horizontal and vertical velocities of the CYPOS GNSS stations in IGB08 (values in mm/yr).

	Validity period	Vnorth	Veast	Vup
EVRY	A	14.7	19.5	0.2
LARN	A	13.6	20.2	-4.9
LEFK	B	16.3	19.3	0.1
	C	16.4	19.3	0.2
LEME	A	15.6	20.3	0.3
NICO	A	15.7	18.9	-0.3
PAFO	D	16.1	19.6	1.7
	E	15.9	19.7	1.6
PARA	A	17.2	18.9	0.6
POLI	A	14.2	19.1	-0.4

(*) The following time periods apply to the above results:
 A: 30/11/2011 - 28/01/2017, D: 30/11/2011 - 9/3/2016,
 B: 30/11/2011 - 21/3/2013, E: 10/3/2016 - 28/1/2017,
 C: 22/3/2013 - 28/1/2017

C. Quality assessment

To give a general overview of the quality of the multi-year solution, the coordinate repeatability for all network stations is depicted in Figure 5. In this figure we show the root-mean-square (rms) of the daily residuals at each station (separately for *east*, *north* and *up* component) which have been obtained by the least squares stacking adjustment during the computation of the multi-year solution. These values are less than 1 cm in all stations. The *up* component seems to have 2-3 times larger values than the horizontal components. Note that a significant part of the daily coordinate residuals at the CYPOS stations is attributed to annual periodic signals due to unmodeled loading effects in the GNSS data (see Section III).

As an additional validation for the multi-year solution, we have re-computed the daily coordinates of all network stations in IGB08 via minimally-constrained adjustments of the original daily NEQ. The estimated positions and velocities of the 24 EPN reference stations (as obtained from the multi-year solution) were used to provide the “daily reference coordinates” for applying the NNT condition in all of these adjustments. The square root of the a-posteriori variance factor (weighted rms) of the re-computed daily solutions varied between 1-1.5 mm.

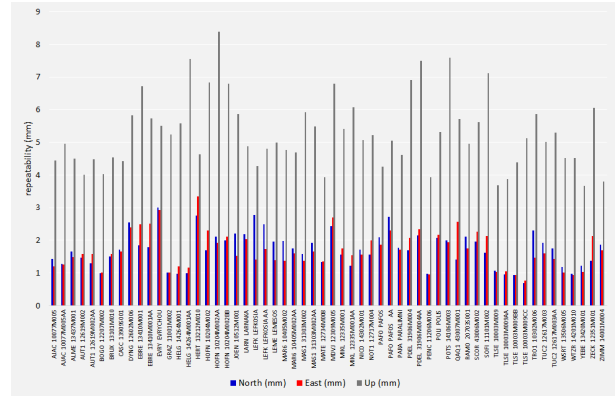


Figure 5. Rms of the coordinate differences btw the daily NEQ solutions and the multi-year solution in the IGB08 frame.

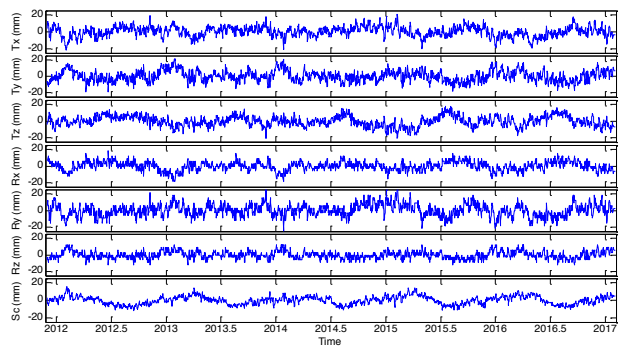


Figure 6. Estimated Helmert parameters btw the re-computed daily solutions and the multi-year solution.

Finally, the re-computed daily solutions were compared with the multi-year solution by a simple least-squares fit using the 7-parameter Helmert transformation. The daily-estimated Helmert parameters are shown in Figure 6, whereas the total rms of the post-fit coordinate residuals is depicted in Figure 7.

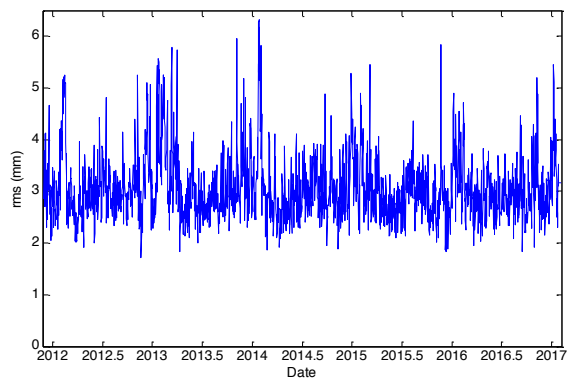


Figure 7. Rms of Helmert transformation residuals btw the re-computed daily solutions and the multi-year solution.

D. Euler pole estimation for Cyprus in IGB08

Using the estimated horizontal velocities of the seven GNSS stations, we have applied the Euler pole model to infer the main parameters of Cyprus’ rotational crustal motion. The least squares estimates of the Euler pole

position (Φ , Λ) and the respective anti-clockwise angular velocity (ω) are given in Table 4.

Table 4. Estimated Euler pole parameters for Cyprus.

Φ (deg.)	Λ (deg.)	Ω (deg./Myr)
49.83 ± 0.34	13.19 ± 0.15	0.629 ± 0.004

The rms of the post-fit station velocity residuals from the aforementioned adjustment was 0.9 mm/yr. Their actual values ranged between 0.1-0.7 mm/yr for the East component, and between 0.2-2.1 mm/yr for the North component. Overall, the post-fit velocity residuals were consistently smaller than 1 mm/yr, with the exception of LARN whose residuals were 2.1 mm/yr and 0.5 mm/yr for the North and East component, respectively.

Based on the previous values, it is concluded that the geographical area covered by the CYPOS GNSS network seems to be rather stable, and it does not show any significant local deformation in the horizontal sense. The station located in Larnaka, however, appears to be affected by localized effects (presently of unknown origin) which influence both the horizontal and vertical components of the respective position time series (see also Table 3).

III. POSITION TIME-SERIES OF CYPOS GNSS STATIONS

A. Station discontinuities

During the computation of the multi-year solution, the time series of daily residuals at each network station were examined to identify possible discontinuities. Two different strategies were applied for this purpose: the first relied on the use of the FODITS script of the Bernese software (Ostini, 2012), whereas the second employed a modified version of the “step detection algorithm” (Blewitt et al., 2013) which is based on the comparison between the magnitude of estimated “steps” in the time series and a predefined threshold value (either 2.5 times the formal daily coordinate precision or 3 mm). Both strategies managed to identify the same number of discontinuities over the network: nine at EPN stations, and two at CYPOS GNSS stations.

The detected discontinuities in the residual position time series of stations refer to: PAFO (10/03/2016) and LEFK (22/03/2013). It should be noted that none of these stations had any GNSS receiver or antenna change during the examined time period.

The discontinuity at the PAFO station is rather small and not visually detectable. Its magnitude is 3.4 mm, 3.0 mm and 5.4 mm for the North, East and Up components, respectively.

The discontinuity at the LEFK station is larger and it affects mostly the East component (17.8 mm), whereas the North and Up components are both affected to a lesser extent by -2.3 mm and 6.8, respectively. It is worth mentioning that the NICO station (which belongs

both to EPN and IGS networks) is located approximately 6 km from the LEFK station, and it does not appear to have any similar offset in its position time series at the same epoch. Hence, the discontinuity at the LEFK station should not probably be linked to local geodynamical activity, but it is likely related to unknown hardware failure for this particular station. The residual position time series of the LEFK station, before and after correcting for the aforementioned discontinuity during the estimation of the multi-year solution, is shown in Figure 8.

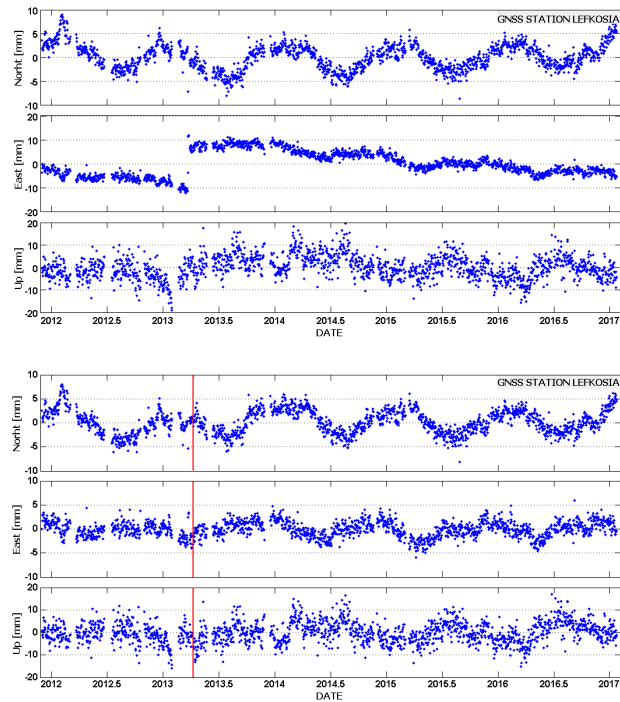


Figure 8. Residual position time series of the LEFK station, before and after the correction of its detected discontinuity.

B. Estimation of periodic signals in position time series of the CYPOS GNSS stations

After the computation of the multi-year solution, the residual time series of daily positions were formed for all network stations. Our focus in this section relies on the temporal behavior (of the topocentric components) of these residual time series at the seven CYPOS stations. Their rms values range from 1.7 mm up to 3 mm for the horizontal components, and from 4.6 mm up to 5.5 mm for the vertical component. Only a portion of these values should be attributed to GNSS data noise, since a large part of the temporal variation in the residual time series is related to systematic effects caused by unmodeled geodynamical processes (non-tidal loading effects).

All permanent GNSS stations in Cyprus show strong annual signals in their position time series, both for the horizontal and vertical components. Such signals originate mostly from unmodeled non-tidal Earth loading effects, and they have a significant impact (of several mm) on the daily station positions. Their characteristic parameters (amplitude, phase) were separately estimated for each topocentric component

through a least squares fit of a simple sinusoidal model to the residual time series of each station. The sinusoidal function that was initially used in these tests contained a mixture of annual and semi-annual periodic terms. However, the estimated parameters of the semi-annual signals were found to be statistically negligible for all stations and, thus, another series of least squares fittings was applied using only annual periodic terms. The respective estimates of the characteristic parameters of the annual signals at the seven CYPOS stations are given in Table 5.

Table 5. Estimated parameters of annual signals in the position time series of CYPOS GNSS stations.

	Amplitude (mm)			Phase (deg)		
	N	E	Up	N	E	Up
EVRY	3.2	3.0	3.2	114.5	80.9	74.0
LARN	2.3	2.1	3.1	253.0	62.2	71.9
LEFK	2.7	1.3	2.4	259.5	344.9	80.6
LEME	2.1	0.6	4.1	45.2	190.0	244.8
PAFO	2.3	1.2	2.2	211.6	49.0	109.0
PARA	1.7	1.3	2.3	233.0	59.9	78.8
POLI	2.0	1.4	2.9	212.7	22.2	79.4

According to Table 5, the amplitudes of the annual signals vary from 0.6 mm to 4.1 mm. The highest value occurs in Up component at the station located in Lemosos (LEME), whereas the same station has the smallest amplitude in the East component (0.6 mm). Note, however, that the daily GNSS data from this particular station cover only a two-year period (2015-2017) and, thus, the estimated annual signals of its topocentric components will not be as accurate compared to the other CYPOS stations – this may also explain the large difference in the estimated phase value for LEME with respect to the rest of the stations (see Table 5). Finally, the stations EVRY and LARN exhibit the highest amplitudes for the annual periodic variation in horizontal position among all other stations.

A series of plots showing the residual position time series with the fitted annual curves at the CYPOS GNSS stations is given in the following figures.

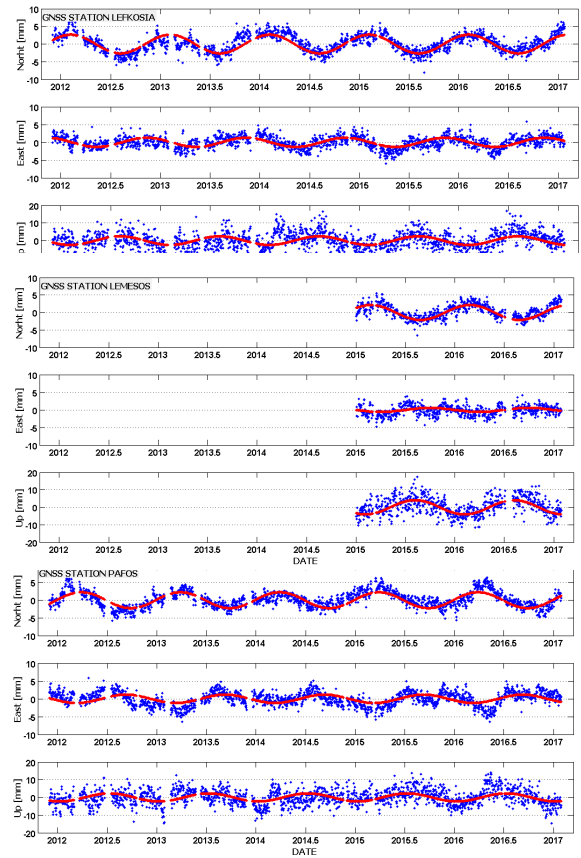
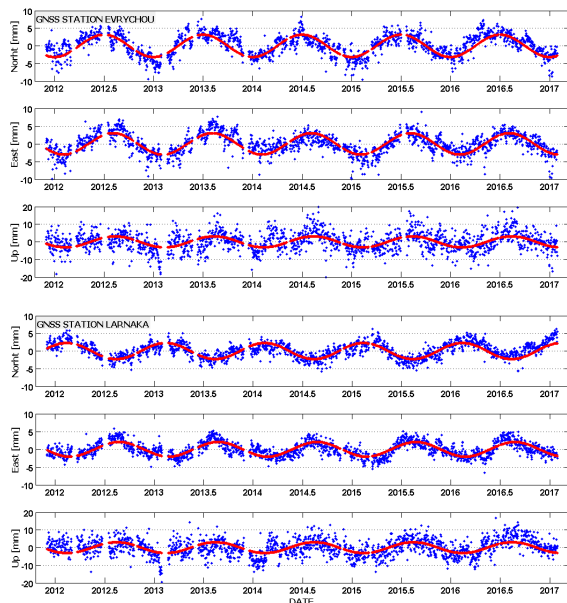


Figure 9. Residual position time series of the CYPOS GNSS stations: EVRY, LARN, LEFK, LEME and PAFO.

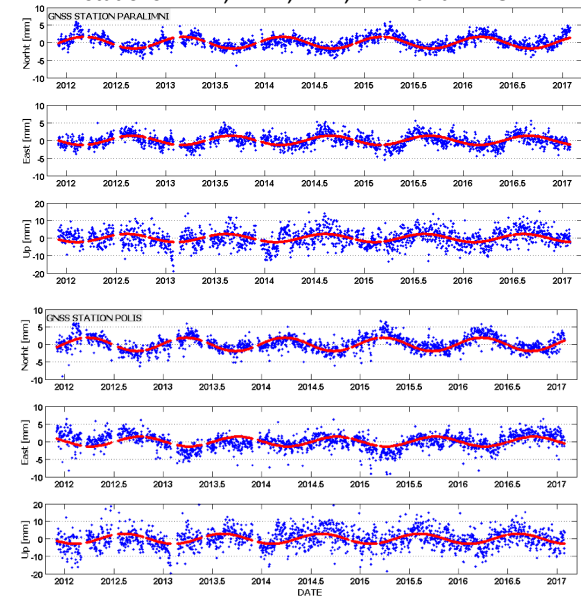


Figure 10. Residual position time series of the CYPOS GNSS stations: PARA and POLI.

The magnitude of the daily post-fit residuals (i.e. after the removal of the estimated annual signals) remains almost the same in all CYPOS stations. Their rms varies between 1-2 mm for the East and North components, and between 4-5 mm for the Up component. Interestingly enough, the temporal behavior of the post-fit residuals is not completely random but it was found to contain additional small signals with periods

lower than 90 days. This particular finding however will not be further analyzed in this paper.

IV. EPILOGUE

The following conclusions can be drawn based on the numerical results of this paper:

- i) the area of Cyprus seems to be stable, without suffering any notable local crustal deformations, at least within the time range considered in the present study (11/2011 - 01/2017);
- ii) the GNSS station that is located in Larnaka (LARN) shows some significant local effects, both in the horizontal and vertical components of its position time series;
- iii) the horizontal and vertical positions of all CYPOS GNSS stations have annual periodic variations of considerable magnitude (several mm) – the semi-annual periodic displacements however were found to be negligible;
- iv) some of the CYPOS GNSS stations appear to have periodic variations in their spatial positions at higher frequencies (120 to 60 days) – the related results have not been presented herein (due to space limitations) and they need to be investigated in detail in the future.

The analysis that was presented in this study will be further continued with the assimilation of additional data from the CYPOS GNSS stations (post-2017) and the implementation of extra processing options (use of the IGS14 reference frame instead of IGB08). Furthermore, the coloured noise characteristics in the derived coordinate time series, in terms of temporal and spatial correlations, will be investigated in a future work.

V. ACKNOWLEDGEMENTS

The data used in this research were kindly provided by the Cyprus Department of Lands and Surveys. The authors would like to specially thank the Director Mr. Andreas Socratous, Dr. Elikkos Elia, Mr Andreas Hadjiraftis, Mrs. Georgia Papathoma, Mr. George Constantinou and Mrs. Nana Mythillou for their assistance and cooperation in the frame of this research endeavor.

References

- Altamimi, Z., L. Métivier, X. Collilieux (2012). ITRF2008 plate motion model. *J. Geophys. Res. Solid Earth* (1978–2012), 117(B7).
- Altamimi, Z., A. Dermanis (2012). The choice of reference system in ITRF formulation. In: N. Sneeuw et al. (eds.), VII Hotine-Marussi Symposium on Mathematical Geodesy, International Association of Geodesy, Symposia 137, pp. 329-334, Springer, Berlin.
- Blewitt, G., C. Kreemer, W.C. Hammond, J.M. Goldfarb (2013). Terrestrial reference frame NA12 for crustal deformation studies in North America. *Journal of Geodynamics*, 72: 11–24.
- Bruyninx, C., Z. Altamimi, A. Caporali, A. Kenyeres, M. Lidberg, G. Stangl, J. Torres (2012). Guidelines for EUREF Densifications. Available at: (ftp://epncb.oma.be/pub/general/Guidelines_for_EUREF_Densifications.pdf).
- Chatzinikos, M. (2013). Study of the earth's crust displacements in the area of Greece analyzing GNSS data. PhD Thesis, School of Rural and Surveying Engineering, Aristotle University of Thessaloniki, Greece.
- Chatzinikos, M., A. Dermanis (2015). A study of the role of the choice of reference system in the analysis of GNSS coordinate time series. Proceedings of the IAG Commission I Symposium, Reference Frames for Applications in Geosciences, Kirchberg, Luxemburg.
- Chatzinikos, M., A. Fotiou, C. Pikridas (2009). The effects of the receiver and satellite antenna phase center models on local and regional GPS networks. Proceedings of the International Symposium on Modern Technologies, Education and Professional Practice in Geodesy and Related Fields, 5 - 6 November, Sofia, Bulgaria.
- Dach, R., S. Lutz, P. Walser, P. Fridez (2015). Bernese GNSS Software Version 5.2. User manual, Astronomical Institute, University of Bern, Bern Open Publishing. doi: 10.7892/boris.72297; ISBN: 978-3-906813-05-9.
- Dach, R., J. Böhm, S. Lutz, P. Steigenberger, G. Beutler (2010). Evaluation of the impact of atmospheric pressure loading modeling on GNSS data analysis. *Journal of Geodesy*, 85: 75–91.
- Dong, D., P. Fang, Y. Bock, M.K. Cheng, S. Miyazaki (2002). Anatomy of apparent seasonal variations from GPS-derived site position time series. *J. Geophys. Res.*, 107(B4), 2075, doi:[10.1029/2001JB000573](https://doi.org/10.1029/2001JB000573).
- Goebell, S., M.A. King (2011). Effects of azimuthal multipath asymmetry on long GPS coordinate time series. *GPS Solutions*, 15: 287–297, doi: 10.1007/s12029-011-0227-7.
- King, M.A., Z. Altamimi, J. Boehm, M. Bos, R. Dach, P. Elsegui, F. Fund, M. Hernández-Pajares, D. Lavallee, P.J.M. Cervera (2010). Improved constraints on models of glacial isostatic adjustment: a review of the contribution of ground-based geodetic observations. *Surv. Geophys.*, 31(5): 465–507. doi:[10.1007/s10712-010-9100-4](https://doi.org/10.1007/s10712-010-9100-4).
- King, M.A., C.S. Watson (2010). Long GPS coordinate time series: multipath and geometry effects. *J. Geophys. Res.*, 115(B4). doi:[10.1029/2009jb006543](https://doi.org/10.1029/2009jb006543).
- Munekane, H., J. Boehm (2010). Numerical simulation of troposphere induced errors in GPS-derived geodetic time series over Japan. *Journal of Geodesy*, 84: 405–417.
- Ostini, L. (2012). Analysis and Quality Assessment of GNSS-Derived Parameter Time Series. PhD thesis of the Philosophisch-naturwissenschaftlichen Fakultät of the University of Bern.
- Penna, N.T., M.A. King, M.P. Stewart (2007) GPS height time series: Short-period origins of spurious long-period signals. *J. Geophys. Res.*, 112, B02402, doi:[10.1029/2005JB004047](https://doi.org/10.1029/2005JB004047).
- Perfetti, N. (2006). Detection of station coordinate discontinuities within the Italian GPS Fiducial Network. *Journal of Geodesy*, 80(7): 381–396.
- Reilinger, R., et al. (2006). GPS constraints on continental deformation in the Africa-Arabia-Eurasia continental collision zone and implications for the dynamics of plate interactions. *J. Geophys. Res.*, 111, B05411.

- Rebischung, P., J. Griffiths, J. Ray, R. Schmid, X. Collilieux, B. Garayt (2011). IGS08: the IGS realization of ITRF2008. *GPS Solutions*, 1–12. doi:10.1007/s10291-011-0248-2.
- Sella, G.F., T.H. Dixon, A. Mao (2002). REVEL: A model for Recent plate velocities from space geodesy. *J. Geophys. Res.*, 107(B4).
- Steigenberger, P., M. Rothacher, M. Fritsche, A. Rülke, R. Dietrich (2009). Quality of reprocessed GPS satellite orbits. *Journal of Geodesy*, 83: 241–248.
- van Dam, T.M., G. Blewitt, M.B. Heflin (1994). Atmospheric pressure loading effects on Global Positioning System coordinate determinations. *J. Geophys. Res.*, 99, 23939–23950.
- van Dam, T.M., J. Wahr (1998). Modeling environment loading effects: A review. *Phys. Chem. Earth*, 23(9–10): 1077-1087, doi:10.1016/S0079-1946(98)00147-5.
- Vey, S., E. Calais, M. Llubes, N. Florsch, G. Woppelmann, J. Hinderer, M. Amalvict, M.F. Lalancette, B. Simon, F. Duquenne, J.S. Haase (2002). GPS measurements of ocean loading and its impact on zenith tropospheric delay estimates: a case study in Brittany, France. *Journal of Geodesy*, 76: 419–427.
- Williams, S. (2003). Offsets in Global Positioning System time series. *J. Geophys. Res.*, 108(B6), doi:[10.1029/2002jb002156](https://doi.org/10.1029/2002jb002156).